

Dynamical simulation on production of W^\pm and Z^0 bosons in pp and Pb–Pb collisions at $\sqrt{s_{\text{NN}}} = 5.02$ TeV with PACIAE

Dai-Mei Zhou^{1, *}, Yu-Liang Yan^{1,2 †}, Liang Zheng^{3, ‡}, Ming-Rui

Zhao², Xiao-Mei Li², Xiao-Ming Zhang¹, Xu Cai¹, and Ben-Hao Sa^{1,2 §}

¹ *Key Laboratory of Quark and Lepton Physics (MOE) and Institute of Particle Physics, Central China Normal University, Wuhan 430079, China.*

² *China Institute of Atomic Energy, P. O. Box 275 (10), Beijing, 102413 China.*

³ *School of Mathematics and Physics, China University of Geosciences (Wuhan), Wuhan 430074, China.*

In this paper, production of W^\pm and Z^0 vector bosons in pp and Pb–Pb collisions at $\sqrt{s_{\text{NN}}} = 5.02$ TeV is dynamically simulated with a parton and hadron cascade model PACIAE. ALICE data of Z^0 production is found to be reproduced fairly well by dynamical simulations with the PACIAE model. A prediction for W^\pm production is given in the same collision systems, at the same energy.

I. INTRODUCTION

W^\pm and Z^0 vector bosons are heavy particles with masses of $m_W = 80.39$ GeV/ c^2 and $m_Z = 91.19$ GeV/ c^2 [1]. They are mainly produced in the large momentum transferred hard partonic scattering processes at the early stage of relativistic pp and Pb–Pb collisions. The main production subprocesses are

$$u\bar{d} \rightarrow W^+, \quad d\bar{u} \rightarrow W^-$$

and

$$u\bar{u} \rightarrow Z^0, \quad d\bar{d} \rightarrow Z^0$$

in leading order approximation [2]. Therefore, the different abundance ratios of valence quarks u and d in pp and Pb–Pb collisions may result in difference on W^+ and W^- production between those two systems. This is the so called isospin effect.

In comparing with evolution time of the heavy-ion collision system, 10 to 100 fm/ c for instance, decay time of W/Z , which can be estimated with the full decay width Γ [1]:

$$t = \frac{\hbar}{\Gamma}, \quad t_W = 0.0922 \text{ fm}/c, \quad t_Z = 0.0791 \text{ fm}/c,$$

is very short. The W/Z leptonic decays

$$W^+ \rightarrow l^+\nu, \quad Z^0 \rightarrow l^+l^-, \quad (l: e, \mu, \tau)$$

are nearly instantaneous. As the produced leptons weakly interact with the partonic and hadronic matters, W^\pm and Z^0 , similar as the prompt direct photon, are powerful probes for investigating the properties of the initial stage of the evolving system and the partonic structure of the colliding nuclei.

Aforementioned properties are in the microscopic sector. In the macroscopic part, for the heavy-ion collisions, the problems to be addressed are geometric properties of the overlapped region of the two colliding nuclei at a given impact parameter b . The key parameters are the nuclear thickness function $\langle T_{\text{AA}} \rangle$ (angle bracket denotes the average over events), the number of participant nucleons $\langle N_{\text{part}} \rangle$, and the number of binary collisions $\langle N_{\text{coll}} \rangle$. They are calculated using the Glauber model [3–6], in which the relation of $\langle N_{\text{coll}} \rangle = \sigma_{\text{NN}}^{\text{inel}} \times \langle T_{\text{AA}} \rangle$ is important.

The CMS and ATLAS Collaborations have first measured W^\pm and Z^0 production in Pb–Pb collisions at $\sqrt{s_{\text{NN}}} = 2.76$ TeV [7–10]. Recently, the ALICE and ATLAS Collaborations published the measurements of Z^0 production at forward rapidities [11] and W^\pm and Z^0 production at mid-rapidity [12, 13], respectively, in Pb–Pb collisions at $\sqrt{s_{\text{NN}}} = 5.02$ TeV. The similar measurement of W^\pm with ALICE is on the way. All those measurements are declared to be well reproduced by the leading-order (LO) and/or next-to-leading-order (NLO) perturbative QCD (pQCD) calculations using the CT14 Parton Distribution Function (PDF) set [14] with and without the parameterized EPPS16 nPDF (nuclear modified Parton Distribution Function) [15]. As the experimental analysis strongly depends on the pQCD assumptions, to only compare data with pQCD predictions is incomprehensive, especially in heavy-ion collisions where the partonic and hadronic scatterings affect also the produced W/Z kinematics. Within this context, studies on W/Z production under the framework considering dynamical properties of the collisions system are particularly important with the fairly accounted initial- and final-state parton showers, multiple parton interactions and semi-hard pQCD processes.

II. MODEL

A parton and hadron cascade model PACIAE [16] is employed in this paper to simulate dynamically Z^0 production in pp and Pb–Pb collisions at $\sqrt{s_{\text{NN}}} = 5.02$ TeV. The results are compared with that measured by AL-

*zhoudm@mail.cnu.edu.cn

†yanyl@ciae.ac.cn

‡zhengliang@cug.edu.cn

§sabh@ciae.ac.cn

ICE [11] for the first time. Production of W^\pm is pre-

dicted under the same conditions as well.

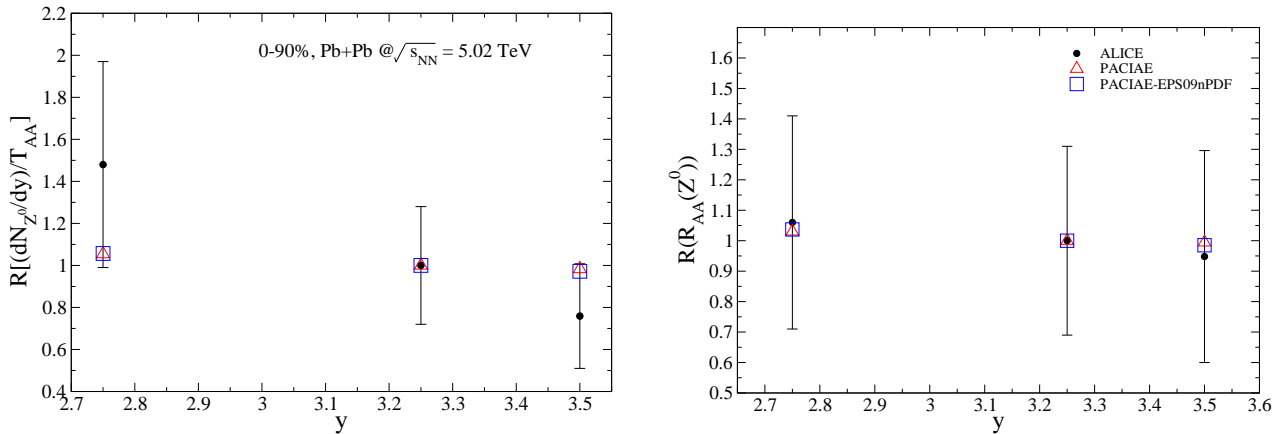


FIG. 1: The left panel is the ratio of $\langle T_{AA} \rangle$ normalized Z^0 differential yield at each observed point y to a special y point as a function of rapidity y . Three observed y points of 2.75, 3.25, and 3.5 are, respectively, at the middle of y intervals of [2.5,3], [2.5,4] and [3-4]. And the right panel is the corresponding R_{AA} as a function of rapidity y .

The PACIAE model is based on PYTHIA event generator (version 6.4.28) [17]. For pp collisions, with respect to PYTHIA, the partonic and hadronic rescatterings are introduced in PACIAE, before string formation and after the hadronization, respectively. The final hadronic

states are developed from the initial partonic hard scatterings followed by the parton and hadron rescattering stages. Thus, the PACIAE model provides a multi-stage transport description on the evolution of the collision system.

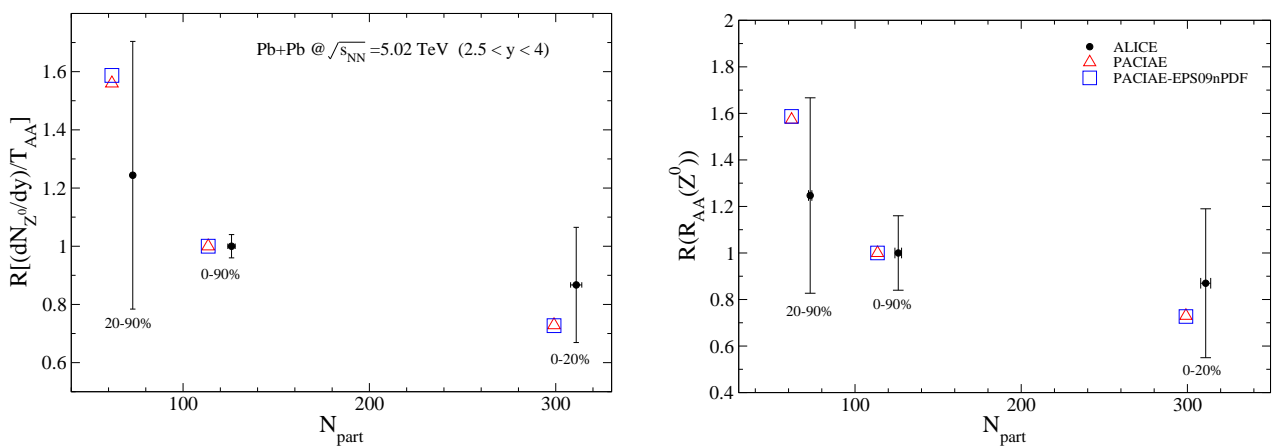


FIG. 2: The same as Fig. (1) but the abscissa now is $\langle N_{part} \rangle$, instead of y in the Fig. (1)

For heavy-ion collisions, the initial positions of nucle-

ons in the colliding nucleus are described by the Woods-

Saxon distribution and the number of participant (spectator) nucleons is determined by the Glauber model [3–6]. Together with the initial momentum setup of $p_x = p_y = 0$ and $p_z = p_{\text{beam}}$ for each nucleon, a list containing the initial state of all nucleons in a given nucleus–nucleus colliding system is constructed.

A collision happened between two nucleons if their relative transverse distance is less than or equal to the minimum approaching distance: $D \leq \sqrt{\sigma_{\text{NN}}^{\text{tot}}/\pi}$. Collision time is calculated with the assumption of straight-line trajectories. All such nucleon pairs compose a nucleon–nucleon (NN) collision (time) list.

A NN collision with least collision time is selected from the list and executed by PYTHIA (using PYEVNW subroutine) with the hadronization temporarily turned-off and the strings as well as diquarks broken-up. The nu-

cleon list and NN collision list are then updated. A new NN collision with least collision time is selected from the updated NN collision list and executed by PYTHIA. Such a routine is repeated until the NN collision list is empty.

With those procedures, the initial partonic state for a nucleus–nucleus collision is constructed. Then it proceeds into a partonic rescattering (cascade) stage where the LO-pQCD parton-parton cross section [18, 19] is employed. After partonic rescatterings, the string is recovered and then hadronized with the Lund string fragmentation model, resulting in an intermediate hadronic state. Finally, the system proceeds into the hadronic rescattering (cascade) stage and results in the final hadronic state of the collisions.

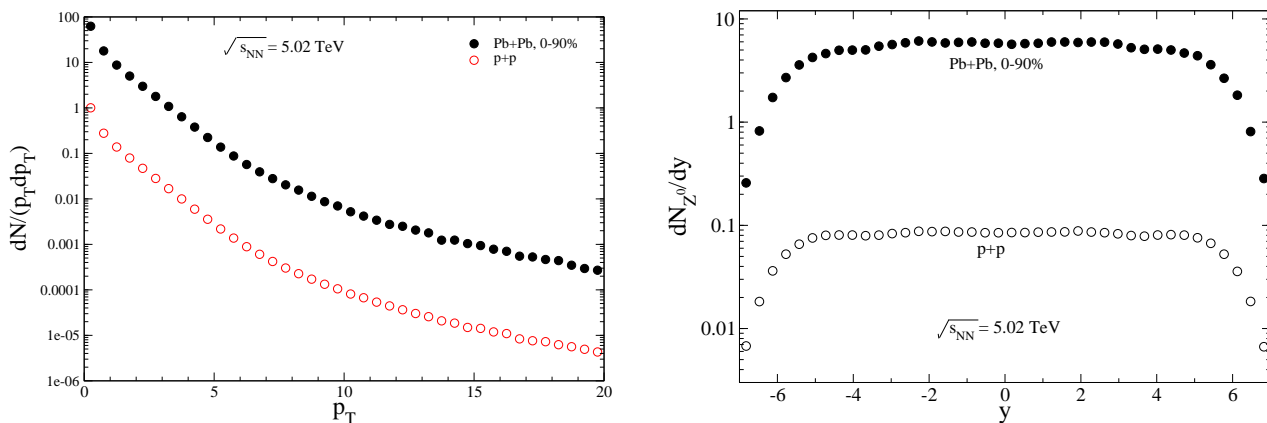


FIG. 3: The transverse momentum distribution (left panel) and rapidity distribution (right panel) of the Z^0 boson in $p + p$ and 0-90% central $Pb + Pb$ collisions at $\sqrt{s_{\text{NN}}}=5.02$ TeV. They are dynamically simulated by PACIAE with EPS09 nPDF.

The W/Z production yield is very low, e.g., $dN(Z^0)/dy \sim 10^{-9}$ at mid-rapidity in the most 20% central Pb–Pb collisions at $\sqrt{s_{\text{NN}}} = 5.02$ TeV. We have to adopt the full user selection for PYTHIA subprocesses. I. e. we set MSEL=0 with

$$\begin{aligned}
 f_i \bar{f}_j &\rightarrow W^+/W^- \\
 f_i \bar{f}_j &\rightarrow gW^+/W^- \\
 f_i \bar{f}_j &\rightarrow \gamma W^+/W^- \\
 f_i g &\rightarrow f_k W^+/W^- \\
 f_i \bar{f}_j &\rightarrow Z^0 W^+/W^- \\
 f_i \bar{f}_i &\rightarrow W^+ W^-
 \end{aligned}$$

for W^\pm production, and with

$$\begin{aligned}
 f_i \bar{f}_i &\rightarrow \gamma^*/Z^0 \\
 f_i \bar{f}_i &\rightarrow g(\gamma^*/Z^0) \\
 f_i \bar{f}_i &\rightarrow \gamma(\gamma^*/Z^0) \\
 f_i g &\rightarrow f_i(\gamma^*/Z^0) \\
 f_i \bar{f}_i &\rightarrow (\gamma^*/Z^0)(\gamma^*/Z^0) \\
 f_i \bar{f}_j &\rightarrow Z^0 W^+/W^-
 \end{aligned}$$

for Z^0 production. In aforementioned equations the f refers to fermion (quark) and its subscript stands for flavor code. Besides, W^\pm and Z^0 are forbidden to decay in the simulations.

The per-event W/Z multiplicity density $dN(W/Z)/dy$ is biased by the selected subprocesses. To compare simu-

lation results with data, a rescaled distribution is defined

$$R(X) = X/X_{\text{ref}}, \quad (1)$$

where X denotes a given observed distribution, such as the normalized per-event multiplicity density $\frac{dN/dy}{T_{AA}}$ or

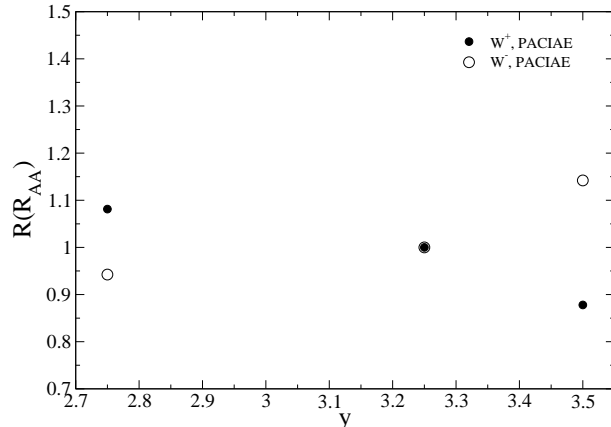
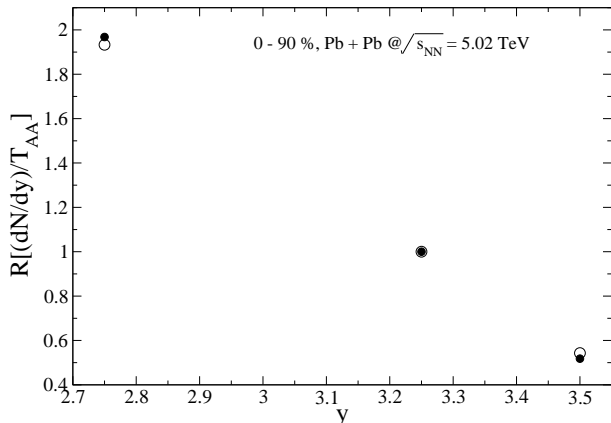


FIG. 4: The same as the Fig. (1) but for W^\pm production by PACIAE model with EPS09nPDF.

III. RESULTS AND DISCUSSIONS

The comparison of the rescaled Z^0 multiplicity density $R(\frac{dN_{Z^0}/dy}{T_{AA}})$ vs. y for 0–90% centrality class in Pb–Pb collisions at $\sqrt{s_{NN}} = 5.02$ TeV between PACIAE dynamical simulations and the ALICE measurements is shown in the left panel of Fig. (1). From the left to the right, the points on the plot represent the results in rapidity intervals of $2.5 < y < 3$, $2.5 < y < 4$ and $3 < y < 4$. In both data and the simulation, the value in $2.5 < y < 4$ is chosen as the reference. The right panel of Fig. (1) shows the comparison of $R(R_{AA}(Z^0))$ vs. y between PACIAE and ALICE measurement under the same conditions as the left panel. In this figure, the black full circles with error bars are the ALICE data [11], the red open triangles are PACIAE results with free proton PDF, and the blue open squares are PACIAE results with EPS09 nPDF [20]. While the EPPS16 uncertainty bands are clearly wider, the differences between the central value of EPPS16 and EPS09 are relatively small. [15]. It shows that the measured $R(\frac{dN_{Z^0}/dy}{T_{AA}})$ is well reproduced by PACIAE dynamical simulations within errors. However, the measured $R(\frac{dN_{Z^0}/dy}{T_{AA}})$ exhibits stronger y dependence than PACIAE predictions. This has to be studied further.

The comparisons of $R(\frac{dN_{Z^0}/dy}{T_{AA}})$ and $R(R_{AA}(Z^0))$ as a function of $\langle N_{\text{part}} \rangle$ between ALICE measurements and

the nuclear modification factor R_{AA} , X_{ref} is a chosen reference in the distribution. The comparison between data and simulations will be presented on the rescaled distribution $R(X)$.

PACIAE simulations are shown, respectively, in the left and right panels of Fig. (2). The same as Fig. (1), the results are obtained in Pb–Pb collisions at $\sqrt{s_{NN}} = 5.02$ TeV. The result for 0–90% centrality class is used as the reference. In both cases, PACIAE simulations reproduce well the ALICE measurements within uncertainties. The little discrepancy on $\langle N_{\text{part}} \rangle$ between data and PACIAE simulations might be attributed to the differences on algorithms in Glauber model calculations (Monte-Carlo Glauber is used by ALICE and optical Glauber is used in PACIAE) and on $\sigma_{NN}^{\text{inel}}$ values used by ALICE and that in PACIAE simulations. The impact parameter interval for each corresponding centrality class has been set to the same as that used by ALICE [5]. Its value is also consistent among the CMS, ATLAS and ALICE Collaborations.

In Fig. (3), the comparisons of transverse momentum (left panel) and rapidity (right panel) distributions of Z^0 bosons in 0–90% Pb–Pb collisions (black solid circles) at $\sqrt{s_{NN}} = 5.02$ TeV to that in pp collisions (red open circles) at the same center-of-mass energy are presented. As expected, both p_T and y distributions between the two collision systems are similar.

Meanwhile, the PACIAE predictions on the observables presented in Fig. (1) and (2) for W^\pm bosons are performed. The results with EPS09 nPDF are given in Fig. (4) and Fig. (5), respectively. In these figures the black full circles are W^+ results and black open

circles are W^- results. The asymmetry of W^+ and W^- production, stemming from the isospin effect, is estimated with the yields in 0-90% Pb-Pb collisions at $\sqrt{s_{NN}} = 5.02$ TeV

$$A_W = \frac{Y_{W^-} - Y_{W^+}}{Y_{W^-} + Y_{W^+}} = 0.0227. \quad (2)$$

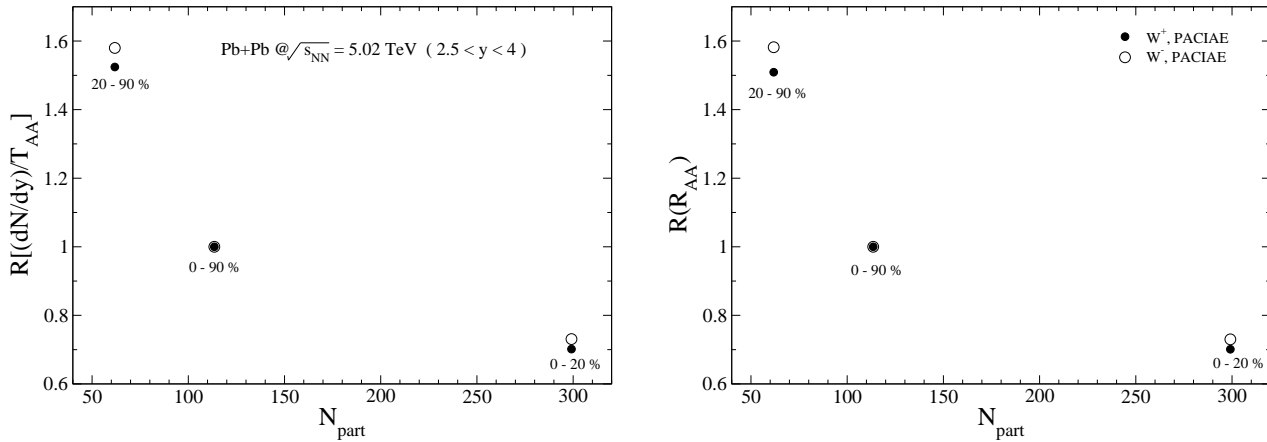


FIG. 5: The same as the Fig. (2) but for W^\pm production by PACIAE model with EPS09 nPDF.

Fig. (6) shows the PACIAE predictions on the transverse momentum (left panel) and rapidity (right panel) distributions of W^\pm in pp and in 0-90% Pb-Pb collisions at $\sqrt{s_{NN}} = 5.02$ TeV. Here, the blue full circles

and red open circles (blue open triangles and blue full triangles) are for W^+ (W^-) in Pb-Pb and pp collisions, respectively. It shows again the similarity in p_T and y distributions between two collision systems, respectively.

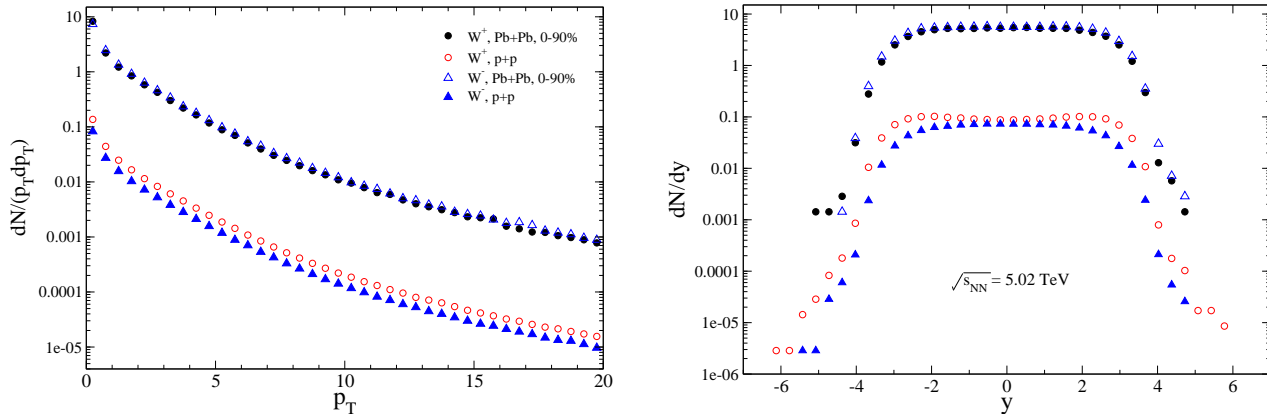


FIG. 6: The transverse momentum distribution (left panel) and rapidity distribution (right panel) of the W^\pm boson in $p + p$ and 0-90% central $Pb + Pb$ collisions at $\sqrt{s_{NN}}=5.02$ TeV. They are dynamically simulated by PACIAE with EPS09 nPDF.

IV. SUMMARY AND ACKNOWLEDGMENT

The parton and hadron cascade model of PACIAE is employed simulating dynamical production of W/Z -

boson in pp and Pb-Pb collisions at $\sqrt{s_{NN}} = 5.02$ TeV

in this paper. The rescaled $\frac{dN/dy}{T_{AA}}$ and R_{AA} for Z^0 bosons measured by ALICE in the pp and Pb–Pb collisions [11] are fairly reproduced. Predictions on W^\pm production is given in the same collision systems and at the same center-of-mass energy. A small W^\pm production asymmetry of 0.0227 is predicted. The effects of initial- and final-state parton showers as well as that of multiple parton interactions on the vector boson production will be

further studied in the next step.

We thank Gang Chen for discussions. This work was supported in part by the National Key Research and Development Project (2018YFE0104800, 2016YFE0100900) and the 111 project of the foreign expert bureau of China as well as by the Science Foundation of China under grant Nos. of 11775094 and 11775313.

-
- [1] Particle data group, Review of Particle Physics, Chinese Phys. C 38 (2014) 27.
- [2] A. D. Martin, R. G. Roberts, W. J. Stirling and R. S. Thorne, Eur. Phys. J. C 14 (2000) 133, arXiv: hep-ph/9907231 [hep-ph].
- [3] A. Shor and R. Longacre, Phys. Lett. B 218, 100 (1989).
- [4] B. I. Abelev, et al., STAR Collaboration, Phys. Rev. C 79, 034909 (2009).
- [5] B. I. Abelev, et al., ALICE Collaboration, Phys. Rev. C 88, 044909 (2013).
- [6] D. Miskowiec, <http://www.linux.gsi.de/~misko/overlap/>.
- [7] CMS Collab., Phys. Lett. B 715 (2012)66, arXiv: 1205.6334 [hep-ex].
- [8] ATLAS Collab., Eur. Phys. J. C 75 (2015) 23, arXiv: 1408.4674 [hep-ex].
- [9] CMS Collab., Phys. Rev. Lett. 106 (2011) 212301, arXiv: 1102.5435 [hep-ex].
- [10] ATLAS Collab., Phys. Rev. Lett. 110 (2013) 022301, arXiv: 1210.6486 [hep-ex].
- [11] ALICE Collab., Phys. Lett. B 780 (2018)372, arXiv: 1711.10753v2 [hep-ex].
- [12] ATLAS Collab., arXiv: 1907.10414v1 [hep-ex].
- [13] ATLAS Collab., arXiv: 1910.13396v1 [hep-ex].
- [14] S. Dulat, T.-J. Hou, J. Gao, M. Guzzi, J. Huston, P. Nadolsky, J. Pumplin, C. Schmidt, D. Stump, and C. P. Yuan, Phys. Rev. D 93 (2016) 033006, arXiv: 1506.07443v2 [hep-ph].
- [15] K. J. Eskola, P. Paakkinen, H. Paukkunen, and C. A. Salgado, Eur. Phys. J. C 77 (2017) 163, arXiv: 1612.05741 [hep-ph].
- [16] Ben-Hao Sa, Dai-Mei Zhou, Yu-Liang Yan, Xiao-Mei Li, Shene-Qin Feng, Bao-Guo Dong, and Xu Cai., Comput. Phys. Commun. 183, 333 (2012); *ibid*, 224, 412 (2018).
- [17] T. Sjöstrand, S. Mrenna, and P. Skands, J. High Energy Phys. 05, 026 (2006).
- [18] B. L. Combridge, J. Kripfgang, and J. Ranft, Phys. Lett. B 70, 234 (1977).
- [19] R. D. Field, Application of perturbative QCD, Addison-Wesley Publishing Company, Inc., 1989.
- [20] L. Helenius, K. J. Eskola, H. Honkanen, and A. Salgado, JHEP, 07, 073 (2012).